THE ATRIUM, SOUTHERN GATE, CHICHESTER, WEST SUSSEX P019 8SQ

*****IMMEDIATE RESPONSE REQUIRED*****

Your article may be published online via Wiley's EarlyView® service (http://www.interscience.wiley.com/) shortly after receipt of corrections. EarlyView® is Wiley's online publication of individual articles in full-text HTML and/or pdf format before release of the compiled print issue of the journal. Articles posted online in EarlyView® are peer-reviewed, copy-edited, author-corrected, and fully citable via the article DOI (for further information, visit www.doi.org). EarlyView® means you benefit from the best of two worlds - fast online availability as well as traditional, issue-based archiving.

Please follow these instructions to avoid delay of publication

☐ **READ PROOFS CAREFULLY**

- This will be your only chance to review these proofs**. Please note that once your corrected article is posted online, it is considered legally published, and cannot be removed from the Web site for further corrections.**
- Please note that the volume and page numbers shown on the proofs are for position only.

☐ **ANSWER ALL QUERIES ON PROOFS** (Queries for you to answer are attached as the last page of your proof.)

- List all corrections and send back via e-mail, or mark all corrections directly on the proofs and send the scanned copy via e-mail. Please do not send corrections by fax or in the post. E-mail corrections to: wileyjournals@macmillan-india.co.in

☐ **CHECK FIGURES AND TABLES CAREFULLY**

- Check size, numbering, and orientation of figures.
- All images in the PDF are downsampled (reduced to lower resolution and file size) to facilitate Internet delivery. These images will appear at higher resolution and sharpness in the printed article.
- Review figure legends to ensure that they are complete.
- Check all tables. Review layout, title, and footnotes.

☐ **COMPLETE CTA (if you have not already signed one)**

- Please send a scanned copy with your proofs and post your completed original form to the address detailed in the covering e-mail. **We cannot publish your paper until we receive the original signed form.**

☐ **OFFPRINTS**

- 25 complimentary offprints of your article will be dispatched on publication. Please ensure that the correspondence address on your proofs is correct for dispatch of the offprints. If your delivery address has changed, please inform the production contact to the journal - details in the covering e-mail. Please allow six weeks for delivery.

Additional reprint and journal issue purchases

- Additional **paper reprints** (minimum quantity 100 copies) are available on publication to contributors. Quotations may be requested from mailto:author_reprints@wiley.co.uk. Orders for additional paper reprints may be placed in advance in order to ensure that they are fulfilled in a timely manner on publication of the article in question. Please note that offprints and reprints will be dispatched under separate cover.
- PDF files of individual articles may be purchased for personal use for $25 via Wiley's Pay-Per-View service (see http://www3.interscience.wiley.com/aboutus/ppv-articleselect.html).
- Please note that regardless of the form in which they are acquired, reprints should not be resold, nor further disseminated in electronic or print form, nor deployed in part or in whole in any marketing, promotional or educational contexts without further discussion with Wiley. Permissions requests should be directed to mailto:permreq@wiley.co.uk
- Lead authors are cordially invited to remind their co-authors that the reprint opportunities detailed above are also available to them.
- If you wish to purchase print copies of the issue in which your article appears, please contact our Journals Fulfilment Department mailto:cs-journals@wiley.co.uk when you receive your complimentary offprints or when your article is published online in an issue. Please quote the Volume/Issue in which your article appears.

EQE 719
pp: 1–18 (col.fig.: Nil)
PROD. TYPE: COM
ED: Prakash
PAGN: Prabhu.I – SCAN: Narendra

EARTHQUAKE ENGINEERING AND STRUCTURAL DYNAMICS
Earthquake Engng Struct. Dyn. (in press)
Published online in Wiley InterScience (www.interscience.wiley.com). DOI: 10.1002/eqe.719

Failure of masonry arches under impulse base motion

Laura De Lorenzis[1,‡], Matthew DeJong[2,§] and John Ochsendorf[2,*,†,‡]

[1]*Department of Innovation Engineering, University of Lecce, Lecce, Italy*
[2]*Building Technology Program, Massachusetts Institute of Technology, Cambridge, MA, U.S.A.*

SUMMARY

Recent seismic events have caused damage or collapse of invaluable historical buildings, further proving the vulnerability of unreinforced masonry (URM) structures to earthquakes. This study aims to understand failure of masonry arches—typical components of URM historic structures—subjected to horizontal ground acceleration impulses. An analytical model is developed to describe the dynamic behaviour of the arch and is used to predict the combinations of impulse magnitudes and durations which lead to its collapse. The model considers impact of the rigid blocks through several cycles of motion, illustrating that failure can occur at lower ground accelerations than previously believed. The resulting failure domains are of potential use for design and assessment purposes. Predictions of the analytical model are compared with results of numerical modelling by the distinct element method, and the good agreement between results validates the analytical model and at the same time confirms the potential of the distinct element framework as a method of evaluating complex URM structures under dynamic loading. Copyright © 2007 John Wiley & Sons, Ltd.

Received 10 October 2006; Revised 17 April 2007; Accepted 24 April 2007

KEY WORDS: arch; discrete element modelling; dynamics; limit analysis; masonry

INTRODUCTION

Unreinforced masonry (URM) structures represent a significant portion of the international built inventory, including most of the world's historical constructions. These structures face several causes of distress including material degradation, foundation settlements, structural alterations, and overloading. However, in seismic zones the major threat to their stability generally comes

*Correspondence to: John Ochsendorf, Building Technology Program, Massachusetts Institute of Technology, Cambridge, MA, U.S.A.
†E-mail: jao@mit.edu
‡Assistant Professor.
§Research Assistant.

Contract/grant sponsor: J. William Fulbright Foundation

from earthquakes. This has been exemplified by recent seismic events which caused damage or collapse of invaluable historical buildings, such as the Basilica of Assisi in Italy and the Citadel of Bam in Iran. It is thus necessary to better understand the collapse of masonry structures to protect human life, cultural resources, and regional economies.

Arches, vaults, and domes are typical components of URM historic structures. Their static analysis, as developed by Heyman [1, 2], assumes that (i) masonry has no tensile strength and infinite compressive strength and (ii) sliding failure does not occur. As a consequence, failure of a masonry arch theoretically occurs by formation of a sufficient number of non-dissipative hinges which transform the arch into a mechanism. Stability under a given load solely depends on the geometry of the structure. This approach is essentially a static equilibrium analysis of rigid body mechanisms.

After the fundamental work by Housner [3], a great deal of research has been devoted to the dynamic behaviour of both a single rigid block and an assembly of rigid blocks subjected to ground accelerations. These studies were aimed primarily at the preservation of monumental structures (in particular archaeological remnants), but also at problems such as the design of elevated water tanks or modelling the overturning of furniture during earthquakes [4–11].

Surprisingly, the dynamic analysis of masonry arches has been given little attention in existing research. Several studies have focused on equivalent static analysis, considering the arch subjected to constant horizontal acceleration (first order earthquake simulation) and constant vertical acceleration (gravity) [12, 13], an approach which has also been applied to portal arch frames [14, 15]. Equivalent static analysis is essentially a stability analysis, again solely based on geometry and independent of scale, which determines the minimum constant ground acceleration required to collapse the arch. This value coincides with the minimum peak ground acceleration needed to transform the arch into a mechanism and hence to initiate its motion. For the arch subjected to varying ground acceleration, equivalent static analysis can only predict the onset of motion and therefore gives a lower bound estimate of the safety of the arch.

Oppenheim [5] was the first to apply a truly dynamic analysis to the masonry arch. Extending the previous work by Allen *et al.* [16], he analysed the dynamic response of an arch considered as a rigid body four-link mechanism under a base acceleration impulse. The location of the hinges (and hence the geometry of the four-link mechanism) was established based on equivalent static analysis, and the subsequent motion of the arch was determined through rigid body dynamics. The impulse magnitude-duration failure domain was determined assuming failure during a single cycle of response, in order to avoid the problems associated with impact. A scale effect similar to that predicted by Housner [3] was detected. Clemente [17] followed up on Oppenheim's work by analysing free vibrations and the response to a sinusoidal base acceleration. The analysis was extended to several cycles of response, but the dissipation of energy due to impact was not considered. More recently, DeJong and Ochsendorf [18] compared Oppenheim's solution with a numerical solution obtained with the distinct element method, and found that the former may be unsafe as the arch may survive the first half cycle of motion but fail during the second.

Advances in non-linear finite element modelling have made it an increasingly more appropriate analysis tool for masonry structures, but the more recent application of discrete element modelling inherently captures the discontinuous nature of masonry and allows for fully dynamic analysis with large displacements. Discrete element programs are particularly suitable for masonry structures because they allow the definition of individual blocks within the structure. Constitutive properties of blocks and contacts must be defined. These programs typically solve the equations of motion of each individual block in the system using a time-stepping scheme. Contact forces on each block are

DOI: 10.1002/eqe

assumed to be proportional to the inter-penetration between blocks, which is determined using the input contact stiffness. The out of balance force after each time step is applied to the equations of motion in the next time step, making the magnitude of the time step critical for accurate modelling.

A limited amount of research has been conducted on the applicability of the discrete element method to masonry structures. Winkler *et al.* [6] applied the discrete element method to simulate the response of rigid single blocks and block assemblies subjected to harmonic base motion. The results given by the numerical model were found to be in good agreement with those obtained from laboratory tests and analytical modelling. Similarly, Papantonopoulos [19] demonstrated good correlation between the solutions yielded by the discrete element method and rigid body dynamics for a rocking block subjected to simulated earthquake ground motion. Bićanić *et al.* [20] applied finite element and discrete element methods to model an actual masonry arch bridge which was subjected to vertical loading until failure. Although the problem involved static loading, the authors concluded that discontinuous modelling frameworks provide a viable alternative for evaluating the structural integrity of masonry, and for predicting the ultimate collapse load and failure mechanism. DeJong and Ochsendorf [18] used the discrete element method to simulate the behaviour of the single rocking block, the masonry arch, and the arch on buttresses. Results were compared with analytical solutions where available and good agreement was found.

In this paper an analytical model is proposed, which follows Oppenheim's [5] approach but also tackles the impact problem and hence predicts the behaviour of the arch during subsequent half cycles of motion. The purpose of the analytical model is twofold. First, it provides a more accurate investigation of the failure domain of the masonry arch subjected to a horizontal ground acceleration impulse. Second, it provides an analytical solution which is compared with numerical results obtained using the discrete element method. The goal of this comparison is a first-order verification of discrete element modelling results which would give confidence in the applicability of the method for analysing more complex URM structures. In the process, the capabilities and shortcomings of the analytical model are observed.

DESCRIPTION OF THE ANALYTICAL MODEL

Analysis of the arch as a four-link mechanism

The model considers a bare part-circular arch having centreline radius R, thickness t, and angle of embrace β. The arch is supported at its ends and subjected to horizontal ground acceleration $\ddot{x}_g$. Masonry is considered rigid, with infinite compressive strength and zero tensile strength, and the coefficient of friction of the mortar joints is assumed to be sufficiently high to prevent sliding.

Following Oppenheim's model [5], the motion of the arch with respect to the ground is considered as a mechanism motion (Figure 1), formed by the four-link mechanism ABCDA. Points A, B, C, and D correspond to the hinge locations at the onset of motion determined by equivalent static analysis, and are only functions of t/R and β. In reality, hinge locations would likely change during motion and more than four hinges might even exist at any particular time. However, it is assumed that hinge locations remain constant, allowing the motion to be approximated by a single-degree-of-freedom (SDOF) model. This assumption is appropriate because the goal of the analytical model is not to exactly describe the behaviour of each voussoir of the arch at all moments in time, but rather to understand the global behaviour of the arch and to obtain a first-order determination of the base motion necessary to cause collapse. The validity of this assumption is discussed later.

DOI: 10.1002/eqe

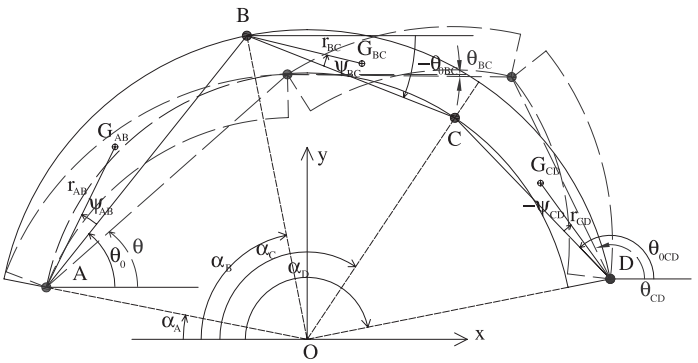

Figure 1. The arch as a four-link mechanism during the first half cycle of motion.

As shown in Figure 1, the mechanism motion is completely described by the rotations of the links θ_{AB}, θ_{BC}, and θ_{CD}, measured counterclockwise from the horizontal. Because the planar four-link mechanism is a SDOF system, one of these rotations (namely $\theta_{AB} = \theta$) is arbitrarily chosen as the Lagrange parameter of the system. Figure 1 marks the link rotations in the initial (undisplaced) configuration of the arch, θ_0, θ_{0BC}, and θ_{0CD}. In the displaced configuration $\theta < \theta_0$, and the variable $\phi = (\theta_0 - \theta) > 0$ will be used to denote rotation with respect to the original geometry.

Displacement analysis and velocity analysis are used to describe the link rotations and rotational velocities, respectively, in terms of θ and $\dot{\theta}$, i.e. to obtain functions $\theta_{BC}(\theta)$, $\theta_{CD}(\theta)$ and $\dot{\theta}_{BC}(\theta, \dot{\theta})$, $\dot{\theta}_{CD}(\theta, \dot{\theta})$. The latter two functions can also be expressed as follows:

$$\dot{\theta}_{BC}(\theta, \dot{\theta}) = \frac{\mathrm{d}\theta_{BC}}{\mathrm{d}\theta}\dot{\theta} = f_{BC}(\theta)\dot{\theta} \tag{1a}$$

$$\dot{\theta}_{CD}(\theta, \dot{\theta}) = \frac{\mathrm{d}\theta_{CD}}{\mathrm{d}\theta}\dot{\theta} = f_{CD}(\theta)\dot{\theta} \tag{1b}$$

For more details, see a standard text on mechanism design and analysis (e.g. [21]).

The differential equation of motion of the system can be derived using Hamilton's principle and Lagrange's equation (see [5] for the details of derivation), and results are as follows:

$$M(\theta)R\ddot{\theta} + L(\theta)R\dot{\theta}^2 + F(\theta)g = P(\theta)\ddot{x}_g \tag{2}$$

where the coefficients $M(\theta)$, $L(\theta)$, $F(\theta)$, and $P(\theta)$ are non-linear in θ and are described further in [5], and g is the acceleration of gravity. Note that Equation (2) does not contain the mass density, which therefore does not affect the behaviour of the system. Conversely, the presence of the average radius R in Equation (2) indicates that a size effect is to be expected.

The initial conditions for Equation (2) are $\theta = \theta_0$ and $\dot{\theta} = 0$ at the start of motion. The equation of motion (2) is valid only for $\theta < \theta_0$. As θ returns to θ_0, the four hinges close and impacts occur. The time interval between the onset of motion and the instant when θ first returns equal to θ_0 is hereafter denoted as time 'before the impact' or the 'first half cycle of motion'. Starting from this instant a different kinematic mechanism governs, which will be analysed in the next subsection.

DOI: 10.1002/eqe

Once θ as a function of time is known by solving Equation (2) with the above initial conditions, the motion of the system before the impact is known.

Mechanism motion after impact

When θ returns equal to θ_0 the four hinges close, impacts occur, and the arch is transformed into a different four-link mechanism which moves in the opposite direction. The geometry of this new mechanism is determined by the location of four new hinges, assumed to form symmetrically with respect to those of the first half cycle of motion (Figure 2). The assumption of symmetric hinges is obviously a simplification of the actual response, again employed to allow the subsequent motion to be described by a SDOF analytical model. Regardless, since the hinge locations are again assumed to remain unchanged after impact, the assumption of symmetric hinge locations provides an appropriate set of 'average' hinge locations for the second half cycle of motion, and is not meant to describe the exact hinge locations after impact. While an analytical solution for the appropriate hinge locations after impact has not been derived, justification for the symmetric hinge location assumption will be presented through comparison with numerical modelling results discussed later.

As shown in Figure 2, all geometric and kinematic quantities in the phase after impact are given the superscript 'prime', and angles are now measured in the opposite direction. The resulting equation of motion is similar in form to Equation (2):

$$M(\theta')R\ddot{\theta}' + L(\theta')R\dot{\theta}'^2 + F(\theta')g = -P(\theta')\ddot{x}_g \tag{3}$$

where the significance of the coefficients is the same as before. The initial conditions for equation (3) are $\theta' = \theta'_0 = \theta_0$ and $\dot{\theta}' = \dot{\theta}'_f$, where $\dot{\theta}'_f$ is the rotational velocity of link $A'B'$ immediately after impact, which must be computed by solving the impact problem described in the next section. Once Equation (3) is solved, the motion of the system after impact is known.

Equation (3) is valid only for $\theta' < \theta'_0$. As θ' returns equal to θ'_0 a new impact occurs and the kinematics of the system change again. Keeping the assumption of the formation of symmetric hinges, the arch re-forms the mechanism of Figure 1. The process repeats itself, with the arch alternating between mechanisms and governing equations of motion after each impact until failure occurs or motion ceases.

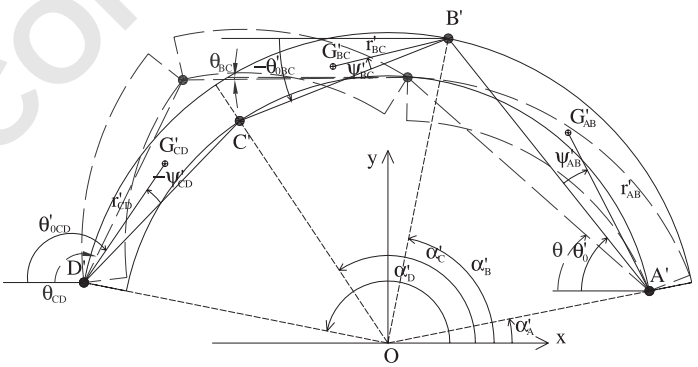

Figure 2. The arch as a four-link mechanism during the second half cycle of motion.

DOI: 10.1002/eqe

Modelling of the impact

Any time the arch returns to its initial undisplaced configuration, an impact occurs and affects the subsequent dynamic behaviour of the system. Figure 3 illustrates the arch at the instant when it returns to its undisplaced configuration after the first half cycle of motion. Solving the impact problem consists of determining the initial conditions for the post-impact motion, using the final conditions (positions and velocities) of the pre-impact motion. For this purpose, suitable simplifying assumptions must be introduced.

It is here assumed that the position of the system does not vary during impact, while its velocities are subjected to an instantaneous variation due to the action of impulsive forces. Impact occurs at the hinge sections, where contact generally involves a finite area which is *a priori* unknown. In analogy with Housner's treatment of impact of the single rocking block [3], the impulsive force at each hinge section is assumed to be located on the opposite side of the hinge across the arch thickness, i.e. at points $\overline{A}$, $\overline{B}$, $\overline{C}$, and $\overline{D}$ (Figure 3).

At the location of the internal hinges B and C, the impact generates internal impulsive forces which balance each other. At the locations of the extreme hinges A and D, external impulsive forces $F_{\overline{A}}$ and $F_{\overline{D}}$ arise. The problem can be formulated considering five unknowns, namely: the x- and y-components of $F_{\overline{A}}$ and $F_{\overline{D}}$ ($F_{\overline{A}x}$,$F_{\overline{A}y}$,$F_{\overline{D}x}$,$F_{\overline{D}y}$), plus the rotational velocity of link $A'B'$ immediately after impact, $\dot{\theta}'_f$. The five equations used to determine these unknowns are:

1. The equation of linear momentum along x for the whole arch:

$$F_{\overline{A}x}\Delta t - F_{\overline{D}x}\Delta t - k'_x\dot{\theta}'_f = -p_{x,i} \tag{4a}$$

2. The equation of linear momentum along y for the whole arch:

$$F_{\overline{A}y}\Delta t + F_{\overline{D}y}\Delta t - k'_y\dot{\theta}'_f = -p_{y,i} \tag{4b}$$

3. The equation of angular momentum about O for the whole arch:

$$-F_{\overline{A}x}\Delta t \cdot y_{0\overline{A}} + F_{\overline{A}y}\Delta t \cdot x_{0\overline{A}} + F_{\overline{D}x}\Delta t \cdot y_{0\overline{D}} + F_{\overline{D}y}\Delta t \cdot x_{0\overline{D}} - k'_O\dot{\theta}'_f = -L_{O,i} \tag{4c}$$

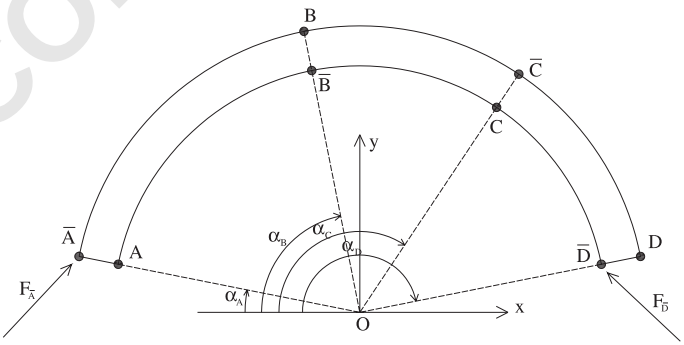

Figure 3. The arch in the instant of the impact.

DOI: 10.1002/eqe

4. The equation of angular momentum about $\overline{B}$ for the portion of the arch on the left of $\overline{B}$:

$$F_{\overline{A}x}\Delta t \cdot (y_{0\overline{B}} - y_{0\overline{A}}) - F_{\overline{A}y}\Delta t \cdot (x_{0\overline{B}} - x_{0\overline{A}}) - k'_{\overline{B}}\dot{\theta}'_f = -L_{\overline{B},i} \tag{4d}$$

5. The equation of angular momentum about $\overline{C}$ for the portion of the arch on the right of $\overline{C}$:

$$-F_{\overline{D}x}\Delta t \cdot (y_{0\overline{C}} - y_{0\overline{D}}) + F_{\overline{D}y}\Delta t \cdot (x_{0\overline{D}} - x_{0\overline{C}}) - k'_{\overline{C}}\dot{\theta}'_f = -L_{\overline{C},i} \tag{4e}$$

where Δt is the duration of the impact, the k'_{-} terms are known geometric coefficients, the $p_{-,i}$ and $L_{-,i}$ terms are known quantities of linear and angular momentum immediately before impact, and the x_{0-} and y_{0-} terms are known x- and y-coordinates of points in the initial (undisplaced) configuration of the arch, respectively. In writing the equations, self-weights are neglected because they are small compared to impulsive forces, as is normally assumed for impact problems. By solving the system of equations, the angular velocity immediately after impact ($\dot{\theta}'_f$) is computed.

Coefficient of restitution

The coefficient of restitution for the impact can be defined with reference to the angular velocity:

$$c_v = \frac{\dot{\theta}'_f}{\dot{\theta}_i} \tag{5}$$

where $\dot{\theta}_i$ is the rotational velocity of link AB immediately before impact, or with reference to the kinetic energy:

$$c_T = \frac{T_f}{T_i} \tag{6}$$

where T_f and T_i are the kinetic energies immediately after and immediately before impact, respectively. As hinges after impact are assumed to form symmetrically to those before impact, T_i and T_f, are, respectively, proportional to $\dot{\theta}_i^2$ and $\dot{\theta}_f'^2$, with the same proportionality coefficient. Hence,

$$c_T = c_v^2 \tag{7}$$

It also results that the coefficient of restitution depends only on the geometry of the arch (t/R, β, and the number of voussoirs) and is independent of scale. As t/R increases or β decreases, the coefficient of restitution decreases, i.e. a larger fraction of the arch kinetic energy is dissipated during the impact.

Clearly, the impact model employed above does not attempt to account for complex impact behaviour such as sliding, slide rocking, or bouncing [7–11]. Incorporating these behaviours in a SDOF analytical arch model is not logical and is not within the scope or the purpose of this paper. Regardless, the impact model *does* provide an effective means of estimating an equivalent coefficient of restitution which describes the impact, which is appropriate for this analytical model, and which is only dependent on the initial geometry. Furthermore, within the same analytical framework a coefficient of restitution could be directly prescribed *in lieu* of solving the impact problem, if desired.

DOI: 10.1002/eqe

PREDICTIONS OF THE ANALYTICAL MODEL

Time history analysis

The model is here applied to the arch considered in the paper by Oppenheim [5], whose geometry is defined by $t/R = 0.15$, $\beta = 157.5°$, $R = 10\,\text{m}$ and which consists of seven voussoirs (also called 'Oppenheim's arch' hereafter), subjected to the same forcing function $\ddot{x}_g$ as in Oppenheim's study. This is an idealized function consisting of a pulse of constant ground acceleration with duration t_p and magnitude a, followed by a pulse in the opposite direction with half of the initial magnitude $(a/2)$ and with twice the duration $(2t_\text{p})$, producing zero terminal ground velocity.

The acceleration required to transform the arch into a mechanism and hence to initiate its motion can be obtained through equivalent static analysis, and for the given values of t/R and β is equal to $-0.37g$. The negative sign is due to the assumed direction for the mechanism during the first half cycle (base motion to the left which yields clockwise arch rotation, Figure 1) combined with the sign convention assumed for x (and hence $\ddot{x}_g$). The arch motion as a function of time is determined by solving Equations (2) and (3) repeatedly until failure occurs or motion stops. The impact model is solved every time ϕ (or ϕ') returns to zero, and failure is identified by an ever-increasing ϕ (or ϕ') during any given half cycle.

Figure 4 shows results for impulses of magnitude $a = 1.0g$ and three different durations. The impulse excitations are shown in Figure 4(a), whereas Figure 4(b)–(d) illustrates the arch response for t_p equal to 0.44, 0.27, and 0.20 s, respectively. For $t_\text{p} = 0.44$ s, the arch fails during the first half cycle of motion and no impact occurs. For $t_\text{p} = 0.27$ s, the arch recovers from the initial half cycle of motion and impact occurs at a time of ~ 0.86 s (at which time the external excitation has ceased already), and failure occurs during the second half cycle of motion as ϕ' increases continuously. For $t_\text{p} = 0.20\,\text{s}$, the arch initially recovers and impact occurs at $\sim 0.6\,\text{s}$ (at which time the external excitation has just ceased), and then recovers from the second half cycle of motion causing a second impact. Although it is not shown, the motion continues with the arch alternating between the two kinematic mechanisms of Figures 1 and 2. Successive half cycles have decreasing amplitude and decreasing duration, until the total kinetic energy is dissipated and the arch returns to rest. This behaviour is in agreement with Housner's findings on the single rocking block [3] as well as observed experimental results for the arch by the authors.

Failure domain

The analysis above was repeated systematically to find the combinations of impulse magnitude and duration leading to arch failure during the first and second half cycles of motion. Results for the sample arch under investigation are reported in Figure 5.

The boundary corresponding to failure during the first half cycle is the same as was determined by Oppenheim [5]. The boundary corresponding to failure during the second half cycle is significantly lower, which indicates that design or assessment of the arch based on single half cycle failure is unsafe. As the impulse duration increases, the magnitudes required to lead the arch to failure during both the first and second half cycles decrease, asymptotically approaching the magnitude required to initiate motion.

The region below $0.37g$ corresponds to impulses which cause no hinges to form; the arch acts as a rigid body and follows the motion of the ground. The region below the lowest curve corresponds to conditions of recovery after the second half cycle of motion; the arch is transformed into a mechanism but survives the first two half cycles of motion. For the shape of impulse considered

DOI: 10.1002/eqe

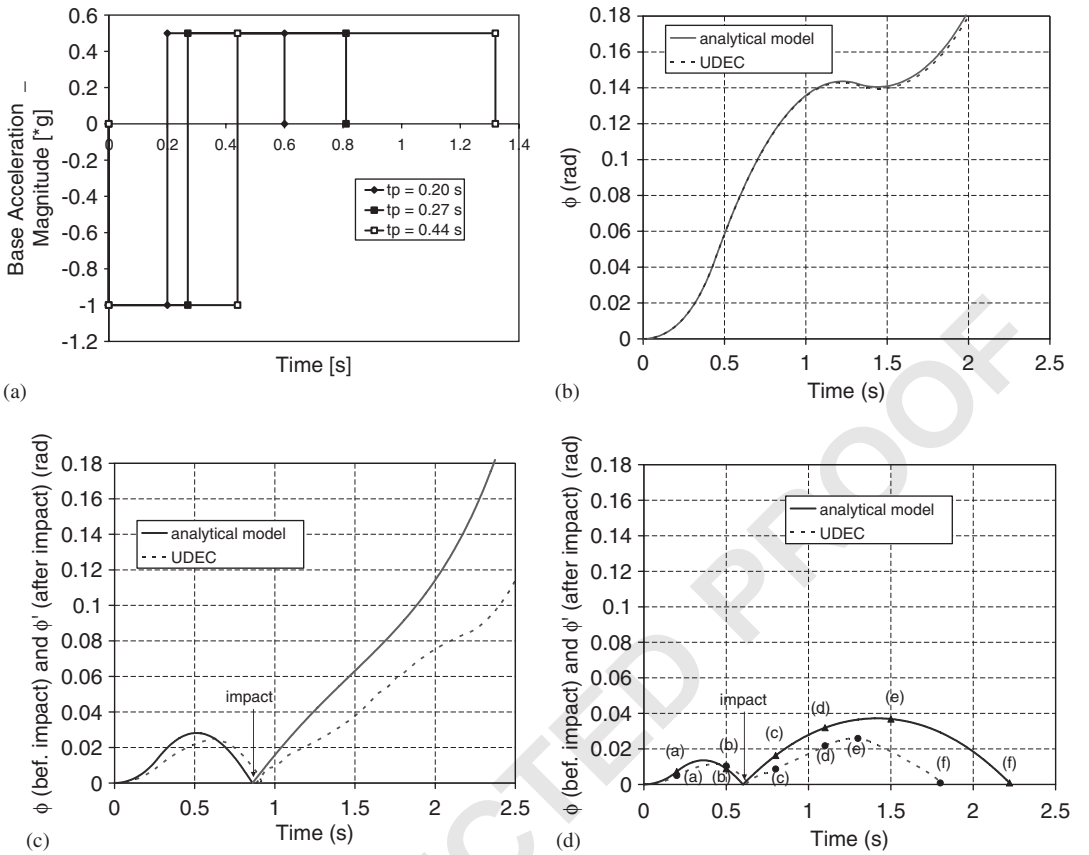

Figure 4. Applied impulses (a) and time histories of mechanism motion for $a = 1.0g$ and $t_p = 0.44$ (b), 0.27 (c), and 0.20 s (d).

here, no collapse occurs during cycles of motion subsequent to the second one, so the arch survives indefinitely. The region between the two curves corresponds to conditions of recovery after the first half cycle but failure during the second half cycle. Finally, excitations in the region above the highest curve lead the arch directly to failure during the first half cycle. The curve to be considered the governing failure domain of the arch is obviously the lowest one, i.e. that corresponding to failure during the second half cycle.

Scale effect

As previously mentioned, the presence of the average arch radius R in the differential equation of motion implies the existence of a scale effect, i.e. arches with the same proportions (t/R ratio and angle of embrace) but different size have different dynamic behaviour and resistance. Figure 6 illustrates the excitation magnitude-duration failure domains for arches of different scales but with $t/R = 0.15$ and $\beta = 157.5°$. The $R = 10$ m arch was analysed in the previous sections.

Figure 6(a) and (b) refers to the domains for failure during the first and the second half cycles of motion, respectively. Both failure domain curves translate upwards as the average radius

DOI: 10.1002/eqe

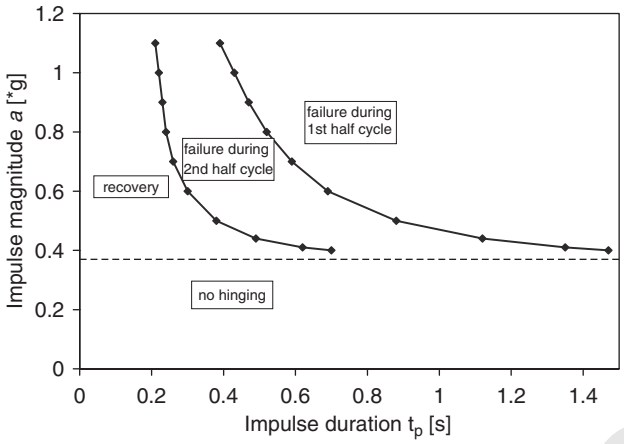

Figure 5. Failure domains of Oppenheim's arch in response to a step impulse function of duration, t_p, and magnitude, a, according to the analytical model.

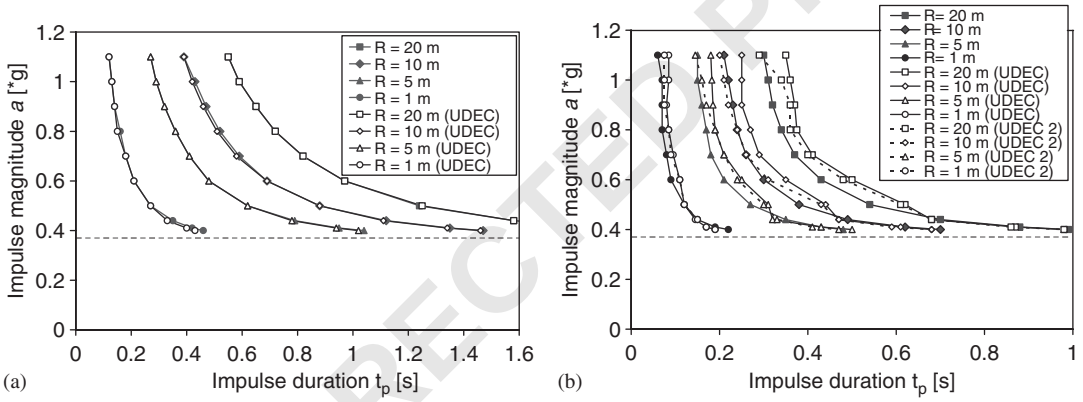

Figure 6. Effect of arch size on the failure domains for the first (a) and second (b) half cycles of motion. UDEC 2 = UDEC with reduced damping parameters ($f_{min} = 0.05$ Hz and $\xi_{min} = 0.001\%$).

increases, i.e. larger arches are more resistant than smaller ones of the same geometric proportions. Furthermore, the failure domain curves are approximately scalable with the square root of the radius. For example, if one of the curves is taken as reference and the impulse magnitude corresponding to a given t_p is multiplied by the square root of the ratio of any desired radius R to the reference radius, the other failure domain curves are obtained. Thus, it is necessary only to compute rigorously the failure domain for an arbitrary reference radius. This confirms both qualitatively and quantitatively the findings of Housner [3].

Effect of arch geometry

Figure 7 illustrates the effect of the arch geometry, in terms of t/R and β, on the excitation magnitude-duration failure domain (corresponding to failure during the second half cycle). As

DOI: 10.1002/eqe

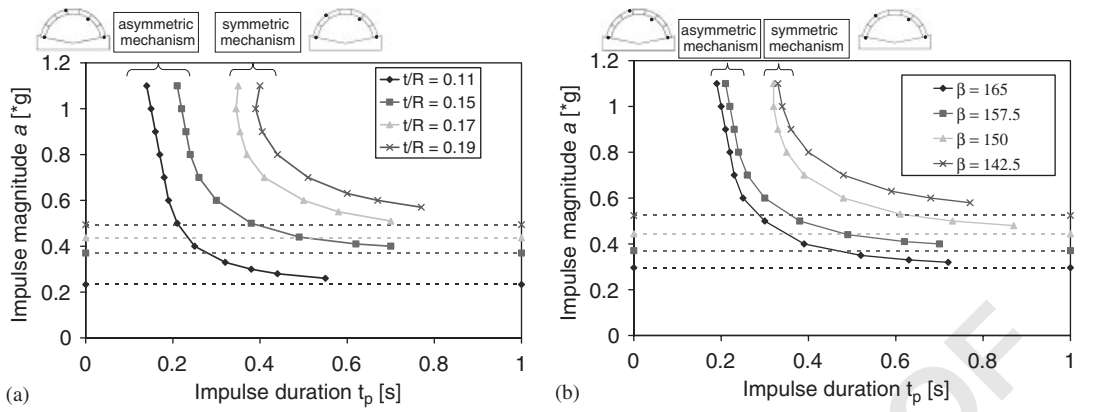

Figure 7. Effect of arch geometry on the failure domain (second half cycle, $R = 10$ m).

expected, increasing the t/R ratio and decreasing the angle of embrace yields an increase in the minimum acceleration needed to initiate motion, and a shift upwards of the entire failure domain, i.e. a greater resistance of the arch to impulse excitation. It also yields a transition in the location of the hinges from asymmetric to symmetric about the y-axis, which does not appreciably affect the shape of the domains but explains their unequal spacing.

The effect of a greater number of voussoirs on the magnitude-duration failure domain was also investigated, and was found to effectively increase the resolution of the possible initial hinge locations which are found using equivalent static analysis. While this does change the four-link mechanism, it has a relatively small effect on the failure domains compared to a change in t/R and β. However, it would reduce the unequal spacing of the failure domains seen in Figure 7.

Line of thrust during motion

At any instant either before or after the impact, the support reactions and the internal compressive forces, i.e. the *line of thrust* [1], of the arch can be calculated by considering the inertia forces and moments acting on the individual links in addition to their self-weight. The line of thrust must be determined based on the deformed configuration of the arch, due to the significant effect of the displacements on the internal forces and moments.

Drawing the line of thrust can give useful information regarding the instantaneous equilibrium conditions of the arch. In particular, the hinge location assumptions of the analytical model can be checked. As mentioned previously, the hinge locations during motion before the impact were assumed to be equal to those at the onset of motion determined through equivalent static analysis. After the impact, new hinges were assumed to form symmetrically with respect to those before the impact. At any given instant, a line of thrust exiting the thickness of the arch would signify the formation of a hinge at that location, suggesting that the actual hinge locations would be different than those assumed.

Figure 8 shows the line of thrust for Oppenheim's arch subjected to an impulse of magnitude $1.0g$ and duration 0.20 s. The arch response for this case was given in Figure 4(d), where the points corresponding to the snapshots of Figure 8 are also marked. The line of thrust evidently exits the thickness of the arch in the first chosen instant of 0.20 s (Figure 8(a)), at which time the first pulse

DOI: 10.1002/eqe

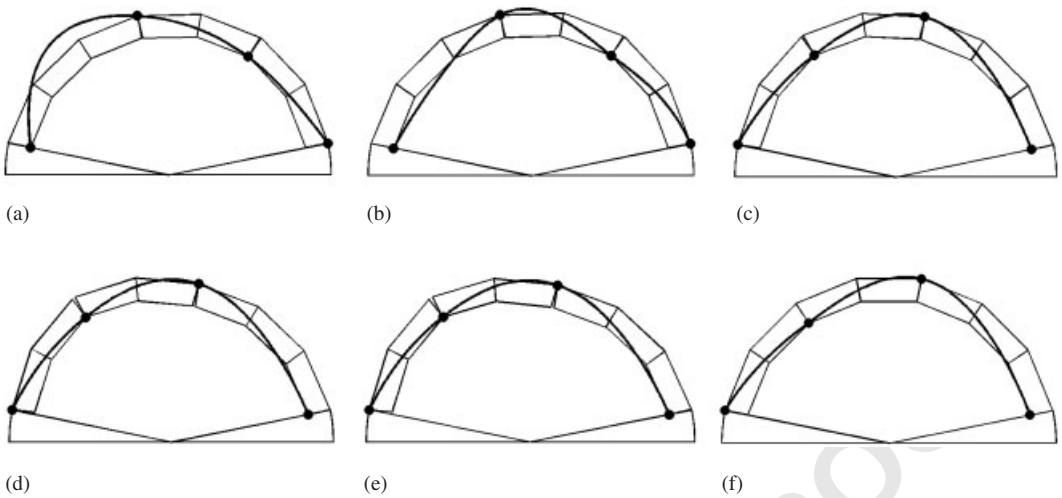

Figure 8. Arch hinge locations and thrust lines found using the analytical model for a step impulse of magnitude $1.0g$ and duration 0.20 s at times: (a) 0.20 s; (b) 0.50 s; (c) 0.80 s; (d) 1.10 s; (e) 1.50 s; and (f) 2.22 s.

is still acting and the arch is undergoing the first half cycle of motion. Although it is not shown, this shape of the line of thrust is representative of the entire time interval during action of the first pulse. In the subsequent instants either during the return pulse (0.50 s, first half cycle of motion, Figure 8(b)) or after the excitation has ceased (second half cycle of motion, Figure 8(c)–(f)), the line of thrust exits the arch thickness at limited locations and by a limited distance, indicating that the assumed hinge locations were quite reasonable.

In principle, the line of thrust could be used to update the location of the hinges during the analysis, by placing the new hinges where the line of thrust has the maximum distance from the axis of the arch. In the case reported in Figure 8(a), the second hinge from left would then be relocated between the second and third voussoirs. The analysis would need to be repeated and the updated line of thrust would possibly suggest a second-iteration location of the hinges. In order to keep the model as simple as possible, this approach was not followed and the hinge location was kept as assumed initially. However, the line of thrust was compared with results of numerical modelling, as will be reported later.

Minimum coefficient of friction to avoid sliding

The computed line of thrust is also valuable for comparing the angle of the line of thrust with respect to the tangential direction of the circular arch centreline. The minimum coefficient of friction required to prevent sliding can then be determined throughout the entire span of the arch at any time throughout motion. For Oppenheim's arch subjected to the impulses in Figure 4(a), the maximum required coefficient of friction always occurs at the right springing (hinge D) at the onset of the impulse ($t = 0^+$), and hence does not depend on the duration of the impulse, but only on the magnitude. For an impulse magnitude of $1.0g$, sliding is prevented if the coefficient of friction is ~ 0.56, which is less than the typical coefficients of friction for masonry. It should be noted that the thrust line at time $t = 0^+$ is not admissible because it exits the thickness of the

DOI: 10.1002/eqe

arch (similar to Figure 8(a)), indicating that hinges actually initially form in different locations. If hinge locations were updated, the minimum coefficient of friction necessary to prevent sliding would be even lower than the one computed above, and hence even closer to the one computed with equivalent static analysis (0.50 for Oppenheim's arch). Regardless, sliding does not occur for the given arch geometry, and the thrust line is shown to be a valuable tool for the necessary check of governing sliding failure.

COMPARISON WITH NUMERICAL RESULTS

Introduction

Analytical results were complemented by a numerical investigation with the discrete element method using the commercial program UDEC [22]. The discrete element method is used to analyse discontinuous materials such as rocks and masonry assemblages. It allows finite displacements and rotations of discrete bodies, including complete detachment, and recognizes new contacts during progression of the analysis. UDEC uses deformable contacts and an explicit, time-domain solution of the governing equations of motion [22, 23].

The masonry arch was considered as an assemblage of rigid blocks with frictional joints. The joint properties required for analysis are the elastic shear and normal stiffnesses, cohesion and friction angle, tensile strength, and dilatancy angle. For consistency with the assumptions of the analytical model, the tensile strength and the cohesion of the joints as well as the dilatancy angle were all taken as zero. The elastic normal and shear stiffnesses were set as 10^{12} GPa/m. The effect of varying the joint stiffnesses was investigated and did not significantly influence failure domain results within a range of 5×10^{11} and 5×10^{12} GPa/m. Lower stiffness values ($<5 \times 10^{11}$ GPa/m) result in contact overlap errors, and higher stiffness values result in excessively small time steps for the solution to remain stable. The friction angle was initially assumed to be very large to ensure that no sliding would occur. Subsequently, the effect of more realistic friction angles was investigated, and is discussed later.

The density of masonry, which was shown not to affect the analytical solution but does affect the numerical solution, was assumed to be 2000 kg/m^3. Finally, numerical dynamic analysis requires definition of the damping ratio. Rayleigh damping ($\alpha = 6.28 \times 10^{-5}$, $\beta = 1.59 \times 10^{-4}$) was used which results in a minimum damping ratio ($\xi_{\min}$) of 0.01% occurring at a frequency ($f_{\min}$) of 0.1 Hz. This limited the damping ratio to less than 0.5% in the frequency range from 0.001 to 10 Hz. The effect of damping is significant and is discussed later.

Motion of the arch

Figure 9 shows the deformed configuration and the hinge locations of Oppenheim's arch subjected to an impulse of magnitude $1.0g$ and duration 0.20 s. The response history for this case is given in Figure 4(d), where the points corresponding to the snapshots of Figure 9 are marked.

In general, the arch motion given by the numerical model agrees with the basic rocking and hinging behaviour predicted by the analytical model. By comparing Figures 8 and 9, the assumptions of the analytical model on the hinge locations can be checked against numerical results. In the first half cycle of motion during action of the first pulse (Figures 8(a) and 9(a)), the location of the second hinge given by the numerical model differs from that given by the analytical model. It is interesting to note that the line of thrust drawn in Figure 8(a) predicts the location of the second

DOI: 10.1002/eqe

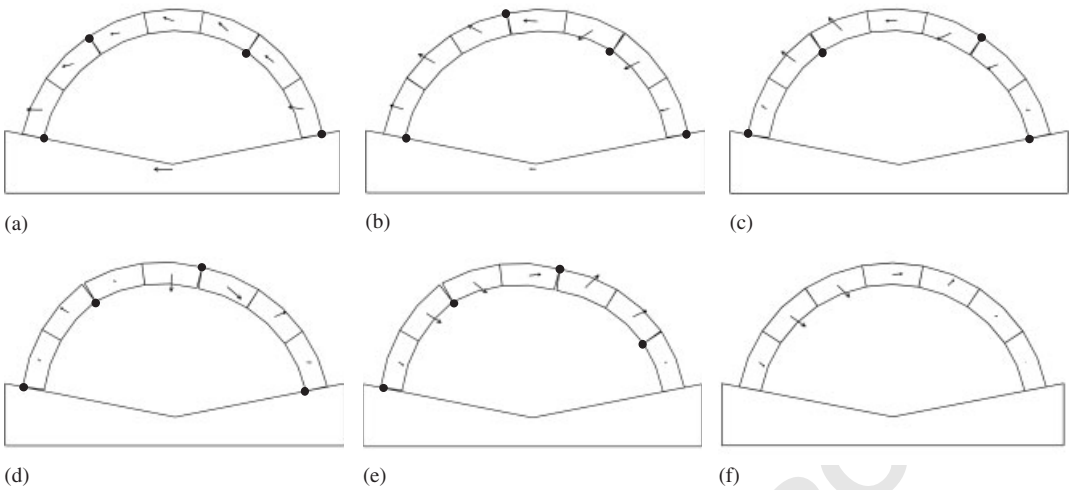

Figure 9. Arch hinge locations and block velocity vectors found using UDEC for a step impulse of magnitude $1.0g$ and duration 0.20 s at times: (a) 0.20 s; (b) 0.50 s; (c) 0.80 s; (d) 1.10 s; (e) 1.30 s; and (f) 1.80 s.

hinge as given by the numerical model. On the other hand, in the first half cycle of motion but during the return pulse (Figures 8(b) and 9(b)), the hinge locations from the two models are the same. After impact, one of the hinges given by the numerical model initially forms at a different location than predicted by the analytical model (0.80 s, Figures 8(c) and 9(c)), then all locations become identical (1.10 s, Figures 8(d) and 9(d)), and finally one hinge in the numerical model changes location again (Figures 8(e) and 9(e)). This demonstrates that while the hinge locations change several times in the numerical model, the hinge locations assumed in the analytical model appear to be appropriate 'average' estimates of the actual hinge locations.

Time history and failure domain

In Figure 4(b)–(d), the response history of the arch as given by the numerical model is compared with analytical predictions. The numerical results plotted in Figure 4(b) are for a three-voussoir arch with the same hinge locations assumed for the analytical model. This was done to verify the accuracy of the analytical and numerical solutions for an identical geometry, and the results show excellent agreement. In Figure 4(c) and (d), the numerical results for the seven-voussoir arch shown in Figure 9 are plotted, and the agreement between the two curves is reasonably good, especially during the pre-impact phase.

The discrepancy between analytical and numerical results comes from two primary sources. First, the hinge locations are not always the same in the two models due to the fact that hinge locations change several times during motion in the numerical model. As a result, the location of the first hinge changes in the numerical model, and affects the angle θ and hence the curve giving ϕ as a function of time. Therefore, the curves in Figure 4(c) and (d) do not actually provide a direct comparison between the analytical and numerical model, but rather an approximate comparison. Second, treatment of the impact conditions by the analytical and numerical models is based on different assumptions, and hence the relative predictions show a more significant discrepancy after

DOI: 10.1002/eqe

impact. The analytical model assumes a single point impact and is based on pure rigid body mechanics, whereas numerical modelling results in several impacts, which occur over a finite contact area having a finite (albeit large) stiffness. Additionally, the energy dissipated during each of these impacts is governed by the specified Rayleigh damping, which is frequency dependent. The stiffness proportional coefficient of Rayleigh damping (β) causes critical damping of high-frequency vibrations (>2000 Hz for the damping specified) which are produced by each impact, causing significant dissipation of energy.

For practical purposes, the most significant predictions are those concerning failure of the arch. Figure 6 compares the excitation magnitude-duration failure domains during the first and second half cycles for Oppenheim's arch, and for arches of different scales, as given by the analytical and numerical models. The agreement is excellent for the first half cycle failure domains, where a three-voussoir arch is again used for numerical modelling and no impacts occur. The agreement between the failure domains during the second half cycle is also quite good considering the simplifications and assumptions which have been made. Moreover, predictions of the analytical model are generally conservative, which results primarily from the fact that the hinge locations may change several times within a single half cycle of motion in the numerical model. As stated earlier, this produces several impacts and hence a greater dissipation of kinetic energy, which in turn explains the smaller rotations (Figure 4) and the greater stability (Figure 6) predicted by the numerical model.

Effect of damping ratio

As mentioned earlier, the damping specified causes significant damping of high-frequency vibrations which result from impacts. However, since the low-frequency damping specified was minimal, very little damping occurs due to the relatively low-frequency rocking motion of the arch. This is exemplified in the results shown in Figures 4(b) and 6(a), where no impacts occurred in both the analytical and numerical models, and the results are almost identical.

In an attempt to evaluate the effect of the damping ratio on the failure domain of the arch as predicted by the numerical model, the domains in Figure 6(b) were recalculated for reduced Rayleigh damping ($\alpha = 6.28 \times 10^{-5}$, $\beta = 1.59 \times 10^{-4}$) resulting in a minimum damping ratio ($\xi_{\min}$) of 0.001% occurring at a frequency ($f_{\min}$) of 0.05 Hz. This limited the damping ratio to less than 0.5% in the frequency range from 5×10^{-5} to 50 Hz. Additionally, it raised the critically damped frequency range from >2000 to $>10\,000$ Hz.

Figure 6 displays the results labelled as 'UDEC 2'. The curves with reduced damping are slightly closer to the analytical failure domains than those with the initial damping parameters. However, the displaced configuration of the arch is no longer characterized by a pure hinging mechanism, as in the previous cases, but also by relative inter-stone displacements similar to those that would be induced by sliding (Figure 10). Note that sliding due to insufficient frictional resistance cannot occur as the friction coefficient assumed in the analysis is unrealistically high.

It is known [24] that high-frequency excitations can cause small inter-stone vibrations that result in irreversible relative displacements of the stones. These relative displacements, which are caused by very brief separation between the stones in masonry structures during vibration, can cause permanent deformation and even collapse. The arch behaviour illustrated in Figure 10 is due to this effect. High-frequency vibrations, which are no longer critically damped due to the reduced damping, cause relative displacements which did not occur with greater damping. In real structures, such high-frequency vibrations are likely to be damped out if there is not

DOI: 10.1002/eqe

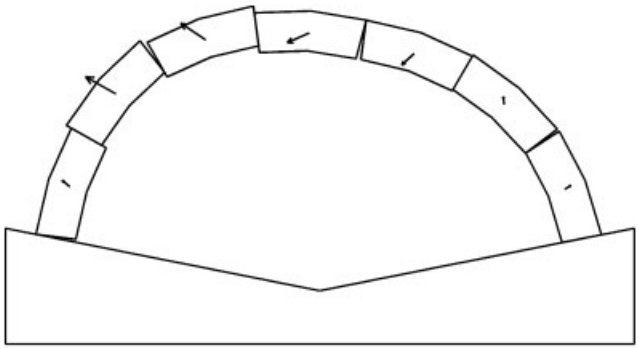

Figure 10. UDEC snapshot of Oppenheim's arch subjected to an impulse of magnitude $a = 1.0g$ and duration $t_p = 0.22$ s at time 1.29 s, with reduced Rayleigh damping ($f_{min} = 0.05$ Hz and $\xi_{min} = 0.001\%$).

a significant high-frequency component in the ground acceleration time history, and hence the previous behaviour was assumed to be unlikely for the assumed impulse excitation. However, for time histories with considerable high-frequency energy, these vibration displacements might be critical. Regardless, the failure domain was not significantly affected for the impulse which was applied.

Effect of friction

The friction angle was initially given a very high value to ensure that no sliding would occur. Subsequently, Oppenheim's arch was subjected to impulses with magnitude-duration combinations corresponding to the failure domains, and the coefficient of friction was gradually lowered to identify the threshold below which sliding occurs. Results were in excellent agreement with predictions of the analytical model. For example, for an impulse magnitude of $1.0g$, the threshold was equal to 0.55, as opposed to the value of 0.56 given by the analytical model. For an impulse magnitude of $0.5g$, the threshold was equal to 0.51 *versus* the value of 0.509 given by the analytical model. Again, this check on friction is imperative to ensure that sliding does not govern failure.

Effect of impulse shape

All results presented thus far have been in response to a step impulse of the form shown in Figure 4(a). However, the same modelling framework can be used to determine the effect of other ground motions as well. For example, single cycle sinusoidal acceleration impulses of period, T, and acceleration magnitude, a, were applied to Oppenheim's arch, resulting in the analytical and numerical failure domains shown in Figure 11. The numerical first half cycle failure domain curve was again found assuming a three-voussoir arch with the same hinge locations used in the analytical model. Analytical and numerical results are almost identical, again verifying that the analytical model was derived correctly. Of more applicable importance, the governing second half cycle failure domain curves also compare quite well, with the analytical model again being slightly conservative. The effect of more complex base motion time histories (e.g. earthquake ground motions) are currently being investigated, but are beyond the scope of this paper. However, at this point it seems likely that numerical modelling will be the more appropriate tool for such

DOI: 10.1002/eqe

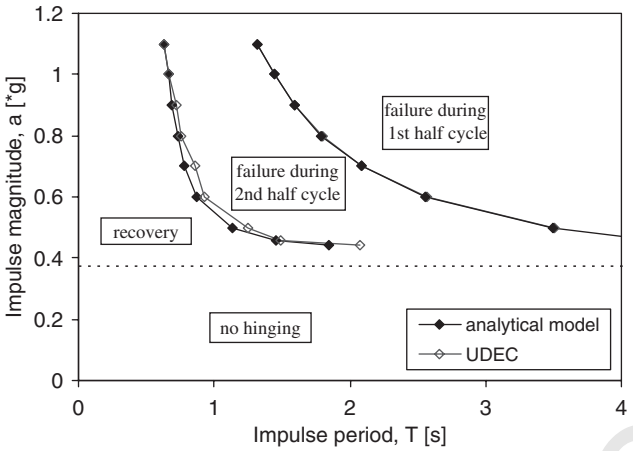

Figure 11. Failure domains of Oppenheim's arch in response to a single cycle sinusoidal impulse function of period, T, and magnitude, a.

analyses as constant hinge location assumptions are likely to break down with longer, more chaotic ground motions.

CONCLUSIONS

In this paper, the behaviour and failure domain of the masonry arch subjected to a ground acceleration impulse have been investigated. Results of analytical and numerical modelling indicate that a SDOF analytical model describes the arch motion quite well and can be used to provide conservative failure domains for design or assessment purposes. Specifically, the following main conclusions are drawn from the combined analytical and numerical approach:

(1) For the assumed shape of impulse, the lowest magnitude-duration failure domain corresponds to failure after impact during the second half cycle of motion. Therefore, this is the governing domain that should be used for design and assessment purposes.
(2) For given geometrical proportions, larger arches are more resistant than smaller ones, by a ratio approximately equal to the square root of the ratio of the arch radii.
(3) For a given size, the resistance of the arch increases as t/R increases or β decreases. The resistance to failure during the second half cycle increases more significantly than resistance to failure during the first half cycle, as the former is also influenced by the energy dissipated during impact.
(4) The minimum coefficient of friction theoretically required to prevent sliding is below the typical values of masonry joints, and hence the assumption of no sliding is reasonable.
(5) Results of numerical modelling of arches subjected to impulse base motion using the distinct element method are in good agreement with analytical results, both in terms of behaviour and failure domain of the arch. This increases the level of confidence in the numerical modelling method, which has potential for the dynamic modelling of more elaborate masonry structures under more complex ground motions.

DOI: 10.1002/eqe

ACKNOWLEDGEMENTS

The first author gratefully acknowledges the J. William Fulbright Foundation for financial support during a research visit to MIT while this work was carried out. Thanks are also extended to Prof. Thomas Peacock for useful discussion, and to the reviewers of this paper whose comments were helpful in improving and clarifying the paper.

REFERENCES

1. Heyman J. The stone skeleton. *International Journal of Solids and Structures* 1966; **2**:249–279.
2. Heyman J. *The Masonry Arch*. Ellis Horwood-Wiley: West Sussex, U.K., 1982.
3. Housner GW. The behavior of inverted pendulum structures during earthquakes. *Bulletin of the Seismological Society of America* 1963; **53**(2):403–417.
4. Augusti G, Sinopoli A. Modelling the dynamics of large block structures. *Meccanica* 1992; **27**(3):195–211.
5. Oppenheim IJ. The masonry arch as a four-link mechanism under base motion. *Earthquake Engineering and Structural Dynamics* 1992; **21**:1005–1017.
6. Winkler T, Meguro K, Yamazaki F. Response of rigid body assemblies to dynamic excitation. *Earthquake Engineering and Structural Dynamics* 1995; **24**:1389–1408.
7. Shenton HW. Criteria for initiation of slide, rock, and slide-rock rigid-body modes. *Journal of Engineering Mechanics* 1996; **122**(7):690-693.
8. Pompei A, Scalia A, Sumbatyan MA. Dynamics of rigid blocks due to horizontal ground motion. *Journal of Engineering Mechanics* 1998; **124**(7):713–717.
9. Andreaus U, Casini P. Dynamics of three rigid block assemblies with unilateral deformable contacts. Part 1: contact modelling. *Earthquake Engineering and Structural Dynamics* 1999; **28**:1621–1636.
10. Andreaus U, Casini P. Dynamics of three rigid block assemblies with unilateral deformable contacts. Part 2: sample application. *Earthquake Engineering and Structural Dynamics* 1999; **28**:1637–1649.
11. Spanos PD, Roussis PC, Politis NPA. Dynamic analysis of stacked rigid blocks. *Soil Dynamics and Earthquake Engineering* 2001; **21**:559–578.
12. Clemente P, Raithel A. The mechanism model in the seismic check of stone arches. In *Arch Bridges*, Sinopoli A (ed.). Balkema: Rotterdam, 1998; 123–129.
13. Ochsendorf JA. Collapse of masonry structures. *Ph.D. Dissertation*, University of Cambridge, Cambridge, U.K., 2002.
14. Baratta A, Zuccaro G, Binetti A. Strength capacity of a no-tension portal arch-frame under combined seismic and ash loads. *Journal of Volcanology and Geothermal Research* 2004; **133**:369–376.
15. De Luca A, Giordano A, Mele E. A simplified procedure for assessing the seismic capacity of masonry arches. *Engineering Structures* 2004; **26**:1915–1929.
16. Allen RH, Oppenheim IJ, Parker AR, Bielak J. On the dynamic response of rigid body assemblies. *Earthquake Engineering and Structural Dynamics* 1986; **14**:861–876.
17. Clemente P. Introduction to dynamics of stone arches. *Earthquake Engineering and Structural Dynamics* 1998; **27**:513–522.
18. DeJong M, Ochsendorf JA. Analysis of vaulted masonry structures subjected to horizontal ground motion. In *Structural Analysis of Historical Constructions*, Lourenco P, Roca P, Modena C, Agrawal S (eds). New Delhi, 2006, in press.
19. Papantonopoulos CL. The earthquake resistance of ancient columns: a numerical perspective developed at the classical temple of Apollo Epikourios. In *Proceedings of the 5th International Conference on Structural Studies, Repairs and Maintenance of Historical Buildings*, Sanchez-Beitia S, Brebbia CA (eds). 1997; 437–446.
20. Bićanić N, Stirling C, Pearce CJ. Discontinuous modelling of masonry bridges. *Computational Mechanics* 2003; **31**:60–68.
21. Erdman A, Sandor G. *Mechanism Design*: *Analysis and Synthesis*. Prentice-Hall: Englewood Cliffs, NJ, 1984.
22. Itasca Consulting Group. *UDEC Version 4.0 User's Guide*, Minneapolis, MN, U.S.A., 2004.
23. Cundall PA, Strack ODL. A discrete numerical model for granular assemblies. *Geotechnique* 1979; **29**:47–65.
24. Meyer P, Germaine J, Kausel E, Ochsendorf J. The impact of high-frequency/low energy seismic waves on unreinforced masonry. *Earthquake Spectra* 2006, accepted for publication.

DOI: 10.1002/eqe

John Wiley & Sons Ltd
The Atrium, Southern Gate, Chichester West, Sussex PO19 8SQ

Author Queries For EQE 719

While preparing this paper/manuscript for typesetting, the following queries have arisen

Query No.	Proof Page/line no	Details required	Authors response
1	Reference	Please provide the publisher name and update Ref. [18].	
2	Reference	Please provide the place of proceedings for Ref. [19].	
3	Reference	Please update Ref. [24].	

COPYRIGHT TRANSFER AGREEMENT

Wiley Production No. .....

Re: Manuscript entitled .....

(the "Contribution") written by .....

(the "Contributor") for publication in.....

(the "Journal) published by John Wiley & Sons Ltd ("Wiley").

In order to expedite the publishing process and enable Wiley to disseminate your work to the fullest extent, we need to have this Copyright Transfer Agreement signed and returned to us with the submission of your manuscript. If the Contribution is not accepted for publication this Agreement shall be null and void.

A. COPYRIGHT

1. The Contributor assigns to Wiley, during the full term of copyright and any extensions or renewals of that term, all copyright in and to the Contribution, including but not limited to the right to publish, republish, transmit, sell, distribute and otherwise use the Contribution and the material contained therein in electronic and print editions of the Journal and in derivative works throughout the world, in all languages and in all media of expression now known or later developed, and to license or permit others to do so.
2. Reproduction, posting, transmission or other distribution or use of the Contribution or any material contained therein, in any medium as permitted hereunder, requires a citation to the Journal and an appropriate credit to Wiley as Publisher, suitable in form and content as follows: (Title of Article, Author, Journal Title and Volume/Issue Copyright © [year] John Wiley & Sons Ltd or copyright owner as specified in the Journal.)

B. RETAINED RIGHTS

Notwithstanding the above, the Contributor or, if applicable, the Contributor's Employer, retains all proprietary rights other than copyright, such as patent rights, in any process, procedure or article of manufacture described in the Contribution, and the right to make oral presentations of material from the Contribution.

C. OTHER RIGHTS OF CONTRIBUTOR

Wiley grants back to the Contributor the following:

1. The right to share with colleagues print or electronic "preprints" of the unpublished Contribution, in form and content as accepted by Wiley for publication in the Journal. Such preprints may be posted as electronic files on the Contributor's own website for personal or professional use, or on the Contributor's internal university or corporate networks/intranet, or secure external website at the Contributor's institution, but not for commercial sale or for any systematic external distribution by a third party (eg: a listserver or database connected to a public access server). Prior to publication, the Contributor must include the following notice on the preprint: "This is a preprint of an article accepted for publication in [Journal title] Copyright © (year) (copyright owner as specified in the Journal)". After publication of the Contribution by Wiley, the preprint notice should be amended to read as follows: "This is a preprint of an article published in [include the complete citation information for the final version of the Contribution as published in the print edition of the Journal]" and should provide an electronic link to the Journal's WWW site, located at the following Wiley URL: http://www.interscience.wiley.com/. The Contributor agrees not to update the preprint or replace it with the published version of the Contribution.
2. The right, without charge, to photocopy or to transmit on-line or to download, print out and distribute to a colleague a copy of the published Contribution in whole or in part, for the Contributor's personal or professional use, for the advancement of scholarly or scientific research or study, or for corporate informational purposes in accordance with paragraph D2 below.
3. The right to republish, without charge, in print format, all or part of the material from the published Contribution in a book written or edited by the Contributor.
4. The right to use selected figures and tables, and selected text (up to 250 words) from the Contribution, for the Contributor's own teaching purposes, or for incorporation within another work by the Contributor that is made part of an edited work published (in print or electronic format) by a third party, or for presentation in electronic format on an internal computer network or external website of the Contributor or the Contributor's employer. The abstract shall not be included as part of such selected text.
5. The right to include the Contribution in a compilation for classroom use (course packs) to be distributed to students at the Contributor's institution free of charge or to be stored in electronic format in datarooms for access by students at the Contributor's institution as part of their course work (sometimes called "electronic reserve rooms") and for in-house training programmes at the Contributor's employer.

D. CONTRIBUTIONS OWNED BY EMPLOYER

1. If the Contribution was written by the Contributor in the course of the Contributor's employment (as a "work-made-for-hire" in the course of employment), the Contribution is owned by the company/employer which must sign this Agreement (in addition to the Contributor's signature), in the space provided below. In such case, the company/employer hereby assigns to Wiley, during the full term of copyright, all copyright in and to the Contribution for the full term of copyright throughout the world as specified in paragraph A above.
2. In addition to the rights specified as retained in paragraph B above and the rights granted back to the Contributor pursuant to paragraph C above, Wiley hereby grants back, without charge, to such company/employer, its subsidiaries and divisions, the right to make copies of and distribute the published Contribution internally in print format or electronically on the Company's internal network. Upon payment of the Publisher's reprint fee, the institution may distribute (but not re-sell) print copies of the published Contribution externally. Although copies so made shall not be available for individual re-sale, they may be included by the company/employer as part of an information package included with software or other products offered for sale or license. Posting of the published Contribution by the institution on a public access website may only be done with Wiley's written permission, and payment of any applicable fee(s).

E. GOVERNMENT CONTRACTS

In the case of a Contribution prepared under US Government contract or grant, the US Government may reproduce, without charge, all or portions of the Contribution and may authorise others to do so, for official US Government purposes only, if the US Government contract or grant so requires. (Government Employees: see note at end.)

F. COPYRIGHT NOTICE

The Contributor and the company/employer agree that any and all copies of the Contribution or any part thereof distributed or posted by them in print or electronic format as permitted herein will include the notice of copyright as stipulated in the Journal and a full citation to the Journal as published by Wiley.

G. CONTRIBUTOR'S REPRESENTATIONS

The Contributor represents that the Contribution is the Contributor's original work. If the Contribution was prepared jointly, the Contributor agrees to inform the co-Contributors of the terms of this Agreement and to obtain their signature(s) to this Agreement or their written permission to sign on their behalf. The Contribution is submitted only to this Journal and has not been published before, except for "preprints" as permitted above. (If excerpts from copyrighted works owned by third parties are included, the Contributor will obtain written permission from the copyright owners for all uses as set forth in Wiley's permissions form or in the Journal's Instructions for Contributors, and show credit to the sources in the Contribution.) The Contributor also warrants that the Contribution contains no libelous or unlawful statements, does not infringe on the right or privacy of others, or contain material or instructions that might cause harm or injury.

Tick one box and fill in the appropriate section before returning the original signed copy to the Publisher

☐ ***Contributor-owned work***

Contributor's signature ..... Date .....

Type or print name and title .....

Co-contributor's signature ..... Date .....

Type or print name and title .....

Attach additional signature page as necessary

☐ ***Company/Institution-owned work (made-for-hire in the course of employment)***

Contributor's signature ..... Date .....

Type or print name and title .....

Company or Institution
(Employer-for Hire) .....

Authorised signature of Employer ..... Date .....

Type or print name and title .....

☐ ***US Government work***

Note to US Government Employees

A Contribution prepared by a US federal government employee as part of the employee's official duties, or which is an official US Government publication is called a "US Government work", and is in the public domain in the United States. In such case, the employee may cross out paragraph A1 but must sign and return this Agreement. If the Contribution was not prepared as part of the employee's duties or is not an official US Government publication, it is not a US Government work.

☐ ***UK Government work (Crown Copyright)***

Note to UK Government Employees

The rights in a Contribution by an employee of a UK Government department, agency or other Crown body as part of his/her official duties, or which is an official government publication, belong to the Crown. In such case, the Publisher will forward the relevant form to the Employee for signature.

WILEY AUTHOR DISCOUNT CARD

As a highly valued contributor to Wiley's publications, we would like to show our appreciation to you by offering a **unique 25% discount** off the published price of any of our books*.

To take advantage of this offer, all you need to do is apply for the **Wiley Author Discount Card** by completing the attached form and returning it to us at the following address:

The Database Group
John Wiley & Sons Ltd
The Atrium
Southern Gate
Chichester
West Sussex PO19 8SQ
UK

In the meantime, whenever you order books direct from us, simply quote promotional code **S001W** to take advantage of the 25% discount.

The newest and quickest way to order your books from us is via our new European website at:

http://www.wileyeurope.com

Key benefits to using the site and ordering online include:

- Real-time SECURE on-line ordering
- The most up-to-date search functionality to make browsing the catalogue easier
- Dedicated Author resource centre
- E-mail a friend
- Easy to use navigation
- Regular special offers
- Sign up for subject orientated e-mail alerts

So take advantage of this great offer, return your completed form today to receive your discount card.

Yours sincerely,

Verity Leaver
E-marketing and Database Manager

*TERMS AND CONDITIONS

This offer is exclusive to Wiley Authors, Editors, Contributors and Editorial Board Members in acquiring books (excluding encyclopaedias and major reference works) for their personal use. There must be no resale through any channel. The offer is subject to stock availability and cannot be applied retrospectively. This entitlement cannot be used in conjunction with any other special offer. Wiley reserves the right to amend the terms of the offer at any time.

REGISTRATION FORM
FOR 25% BOOK DISCOUNT CARD

To enjoy your special discount, tell us your areas of interest and you will receive relevant catalogues or leaflets from which to select your books. Please indicate your specific subject areas below.

Accounting [ ]
- Public [ ]
- Corporate [ ]

Chemistry [ ]
- Analytical [ ]
- Industrial/Safety [ ]
- Organic [ ]
- Inorganic [ ]
- Polymer [ ]
- Spectroscopy [ ]

Encyclopedia/Reference [ ]
- Business/Finance [ ]
- Life Sciences [ ]
- Medical Sciences [ ]
- Physical Sciences [ ]
- Technology [ ]

Earth & Environmental Science [ ]

Hospitality [ ]

Genetics [ ]
- Bioinformatics/Computational [ ]
  Biology [ ]
- Proteomics [ ]
- Genomics [ ]
- Gene Mapping [ ]
- Clinical Genetics [ ]

Medical Science [ ]
- Cardiovascular [ ]
- Diabetes [ ]
- Endocrinology [ ]
- Imaging [ ]
- Obstetrics/Gynaecology [ ]
- Oncology [ ]
- Pharmacology [ ]
- Psychiatry [ ]

Non-Profit [ ]

Architecture [ ]

Business/Management [ ]

Computer Science [ ]
- Database/Data Warehouse [ ]
- Internet Business [ ]
- Networking [ ]
- Programming/Software [ ]
  Development [ ]
- Object Technology [ ]

Engineering [ ]
- Civil [ ]
- Communications Technology [ ]
- Electronic [ ]
- Environmental [ ]
- Industrial [ ]
- Mechanical [ ]

Finance/Investing [ ]
- Economics [ ]
- Institutional [ ]
- Personal Finance [ ]

Life Science [ ]

Landscape Architecture [ ]

Mathematics/Statistics [ ]

Manufacturing [ ]

Material Science [ ]

Psychology [ ]
- Clinical [ ]
- Forensic [ ]
- Social & Personality [ ]
- Health & Sport [ ]
- Cognitive [ ]
- Organizational [ ]
- Developmental and Special Ed [ ]
- Child Welfare [ ]
- Self-Help [ ]

Physics/Physical Science [ ]

[ ] I confirm that I am a Wiley Author/Editor/Contributor/Editorial Board Member of the following publications:

SIGNATURE: .....

PLEASE COMPLETE THE FOLLOWING DETAILS IN BLOCK CAPITALS:

TITLE AND NAME: (e.g. Mr, Mrs, Dr) .....

JOB TITLE: .....

DEPARTMENT: .....

COMPANY/INSTITUTION: .....

ADDRESS: .....

.....

.....

.....

TOWN/CITY: .....

COUNTY/STATE: .....

COUNTRY: .....

POSTCODE/ZIP CODE: .....

DAYTIME TEL: .....

FAX: .....

E-MAIL: .....

YOUR PERSONAL DATA
We, John Wiley & Sons Ltd, will use the information you have provided to fulfil your request. In addition, we would like to:

1. Use your information to keep you informed by post, e-mail or telephone of titles and offers of interest to you and available from us or other Wiley Group companies worldwide, and may supply your details to members of the Wiley Group for this purpose.

   [ ] Please tick the box if you do not wish to receive this information

2. Share your information with other carefully selected companies so that they may contact you by post, fax or e-mail with details of titles and offers that may be of interest to you.

   [ ] Please tick the box if you do not wish to receive this information.

If, at any time, you wish to stop receiving information, please contact the Database Group (databasegroup@wiley.co.uk) at John Wiley & Sons Ltd, The Atrium, Southern Gate, Chichester, West Sussex PO19 8SQ, UK.

E-MAIL ALERTING SERVICE
We offer an information service on our product ranges via e-mail. If you do not wish to receive information and offers from John Wiley companies worldwide via e-mail, please tick the box [ ].

This offer is exclusive to Wiley Authors, Editors, Contributors and Editorial Board Members in acquiring books (excluding encyclopaedias and major reference works) for their personal use. There should be no resale through any channel. The offer is subject to stock availability and may not be applied retrospectively. This entitlement cannot be used in conjunction with any other special offer. Wiley reserves the right to vary the terms of the offer at any time.

Ref: S001W